Measurement 196 (2022) 111270

Contents lists available at ScienceDirect

Measurement

journal homepage: www.elsevier.com/locate/measurement

Reliability of acicular grindable thermocouples for transient temperature measurements at sliding contacts

Oleksii Nosko [a,*], Yurii Tsybrii [a], Wojciech Tarasiuk [b], Andrey Nosko [c]

[a] Gdansk University of Technology, Faculty of Mechanical Engineering and Ship Technology, ul. G. Narutowicza 11/12, Gdansk 80-233, Poland
[b] Bialystok University of Technology, Faculty of Mechanical Engineering, ul. Wiejska 45C, Bialystok 15351, Poland
[c] Bauman Moscow State Technical University, Department of Lifting and Transport Systems, ul. 2-ya Baumanskaya 5, Moscow 105005, Russia

ARTICLE INFO

Keywords:
Sliding contact
Contact temperature
Temperature measurement
Grindable thermocouple
Measurement reliability

ABSTRACT

Acicular grindable thermocouples represent an interesting and prospective technique of temperature measurements at sliding contacts. This study aimed at the investigation of their reliability and accuracy as applied to the friction materials of various classes in contact with steel. The tests were conducted on a pin-on-disc tribometer under stationary and transient regimes. The experimental results were validated by comparing the temperature data obtained by the acicular thermocouple, conventional thermocouples and infrared thermography. It was found that the measurements conducted with the acicular thermocouples are test-retest reliable for copper and a brake pads material, whereas they are not reliable for a polyamide. The temperature rise measured with the acicular thermocouple deviates from that registered by infrared thermography by 7–15% for copper and 10–19% for the brake pads material.

1. Introduction

Thermocouples are commonly used for temperature measurements in the processes related to material removal from the surface of a component, including frictional and machining processes. Since the beginning of the 20th century, several thermocouple techniques have been developed and introduced to tribological applications, as reviewed by Kennedy [1], Komanduri and Hou [2] and Davies et al. [3].

Conventional thermocouples, also referred to as 'embedded thermocouples' in the tribological literature, are one of the earliest thermocouples applied for measuring temperatures in friction components (e.g. Newcomb [4]). A conventional thermocouple is normally installed inside a stationary friction component so that its measuring (hot) junction is located at a small distance from the sliding surface, as schematically shown in Fig. 1a. Apparently, such a thermocouple does not indicate the surface temperature but, rather, a sub-surface one. The inverse heat transfer methods are sometimes used to reconstruct temperature and heat flux at the sliding surface based on the measurements with the conventional thermocouples (Yang and Chen [5], Bauzin et al. [6], Nosko and Tsybrii [7]).

In the dynamic thermocouple technique, the friction components act as the electrodes of the thermocouple, forming the measuring junction directly at their sliding contact (e.g. Bowden and Ridler [8]), as shown in Fig. 1b. Since the measuring junction is composed of actual contact areas, its thickness is microscopically small. As a result, the dynamic thermocouple indicates a higher temperature and its response time is substantially shorter in comparison with the conventional thermocouple. The application region of the dynamic thermocouples is, however, limited to certain combinations of dissimilar pairs of metals.

A modification of the dynamic thermocouple technique has been introduced by Peklenik [9]. An insulated electrode in the form of a wire or foil is installed in a conductive friction component with its end exposed to the sliding surface, whilst the second electrode is the friction component itself, as shown in Fig. 1c. The measuring junction is formed by plastic deformations of the exposed electrode and the adjacent material of the friction component, as the result of their interaction with the counter component. Accordingly, the exposed electrode is being worn out together with the friction component. Since the thermocouples of this type were originally used for measuring temperatures at grinding contacts (Yakimov et al. [10], Tatarenko et al. [11], Lebedev and Zhabokritskiy [12], Karaim [13], Nee and Tay [14], Rowe et al. [15], Babic et al. [16], Batako et al. [17], Lefebvre et al. [18,19], Barczak et al. [20]), they are often referred to as 'single pole grindable thermocouples'.

* Corresponding author.
E-mail address: oleksii.nosko@pg.edu.pl (O. Nosko).

https://doi.org/10.1016/j.measurement.2022.111270
Received 17 January 2022; Received in revised form 22 April 2022; Accepted 25 April 2022
Available online 28 April 2022

Tian et al. [21] and Kennedy et al. [22] reported thin-film thermocouples manufactured on the basis of a physical vapour deposition principle. The electrodes and insulation layers of such a thermocouple represent thin films that are sandwiched to form the measuring junction of microscopic thickness, as shown in Fig. 1d. The thin-film thermocouple enables measuring rapid temperature flashes at a very small contact area, exhibiting outstanding performance. However, the main problem here is that the introduction of the thin films to the friction zone distorts the temperature field under study, i.e. the thin-film thermocouple indicates temperature intrinsic not to the sliding contact between the friction components but to that between its outer insulation layer and the counter component. Besides, accurate vapor deposition of metallic and ceramic films on a substrate is a difficult and resource consuming procedure conducted under strict laboratory conditions.

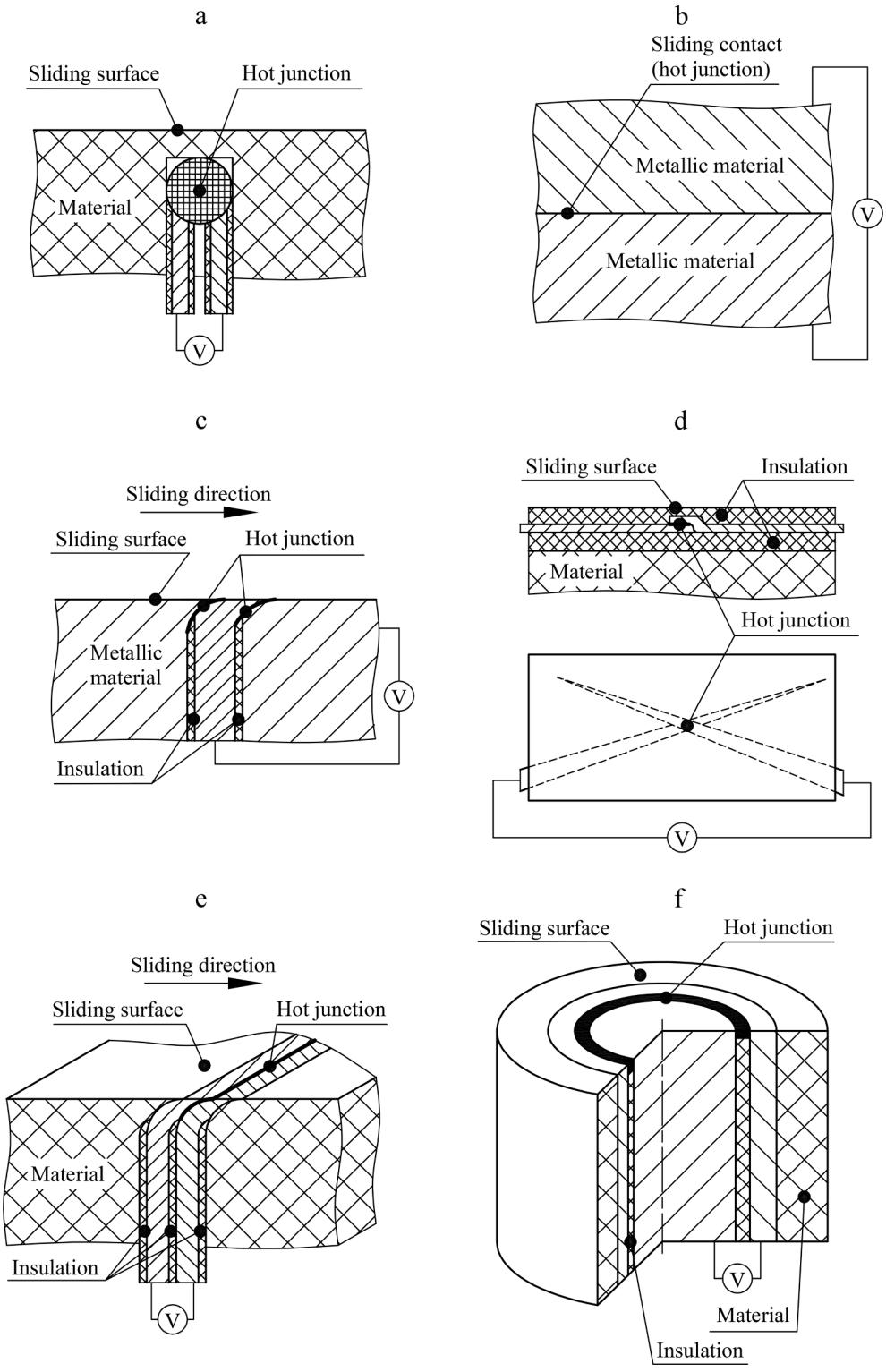

Fig. 1. Types of thermocouples: (a) conventional thermocouple; (b) dynamic thermocouple; (c) single pole grindable thermocouple; (d) thin-film thermocouple; (e) double pole grindable thermocouple; (f) acicular grindable thermocouple.

Another interesting measurement technique utilises double pole grindable thermocouples. In contrast to the single pole grindable thermocouple, the double pole grindable thermocouple includes two parallel electrodes, as shown in Fig. 1e, which makes it applicable to a non-conductive friction component. The ends of its electrodes are exposed to the sliding surface and form the measuring junction by undergoing plastic deformations. Double pole grindable thermocouples have been used for measuring temperatures at sliding contacts, as reported by Guskov [23], Romashko [24], Nee and Tay [14], Nosko and Kimura [25] and Nosko et al. [26]. In the mentioned studies, the thermocouple electrodes represented metallic foils (chromel/alumel, chromel/copel or chromel/constantan) with thickness ranging from 20 μm to about 0.2 mm. Installation of an assembly of two such electrodes requires splitting of the friction component or a piece of it into two parts, which is impractical and substantially narrows the application range of the measurement technique.

An acicular grindable thermocouple shown in Fig. 1f is a double pole grindable thermocouple with a wire-in-hollow-cylinder construction (Nosko et al. [27] and Tarasiuk et al. [28]). Similar thermocouples, although possessing unaltered measuring junctions, are used in aerodynamic and hydrodynamic measurements (Mohammed et al. [29,30], Menezes and Bhat [31], Irimpan et al. [32], Agarwal et al. [33], Desikan et al. [34], Li et al. [35], Manjhi and Kumar [36,37], Rout et al. [38]). The wire-in-hollow-cylinder construction approach allows improving the manufacturability and installation feasibility of the double pole grindable thermocouples and, thereby, opens up new possibilities for their application. With this in mind, the purpose of the present study was to experimentally investigate the reliability and accuracy of the acicular thermocouple technique for the friction materials of various classes under stationary and transient regimes.

2. Research methodology

2.1. Pin-on-disc tribometer

The experiments were performed on a Bruker UMT-2 tribometer equipped with an S23LE rotational motion drive. The pin sample had a cylindrical shape with 8 mm diameter and 8 mm height. The disc sample had diameter 70 mm and thickness 6.5 mm. The average friction radius, i.e. the distance between the axes of the pin and disc samples, was 30 mm. The friction force F was measured by a DFH-20 force sensor with resolution 0.01 N at frequency 10 Hz. The linear wear δ of the pin and disc samples was measured with 1 μm resolution.

2.2. Temperature measurements

The working part of an acicular thermocouple comprises a hollow cylinder electrode, a wire electrode and an insulation layer between the electrodes, as shown in Fig. 1f. The present study investigates the acicular thermocouples with hollow cylinder electrode with 0.34 mm outer diameter and 0.18 mm inner diameter and wire electrode with 0.08 mm diameter. The materials of the hollow cylinder electrode, insulation layer and wire electrode are steel, perfluoroalkoxy and constantan, respectively. More information on the construction, temperature-voltage dependency and other characteristics of the acicular thermocouples can be found in Nosko et al. [27].

The acicular thermocouple was installed in a drilled hole of the pin sample so that the axis of its working part coincided with the axis of the pin sample, as illustrated in Fig. 2. There was an initial gap of about 0.1 mm between the exposed end of the working part (with a premade measuring junction) and the friction surface. The reverse end of the working part was glued to the pin sample. The temperature rise measured by the acicular thermocouple with respect to the environment temperature is denoted by T_{AGT}.

Two conventional K-type thermocouples with bare wire diameter of 0.08 mm were installed in the pin sample. The initial distances between

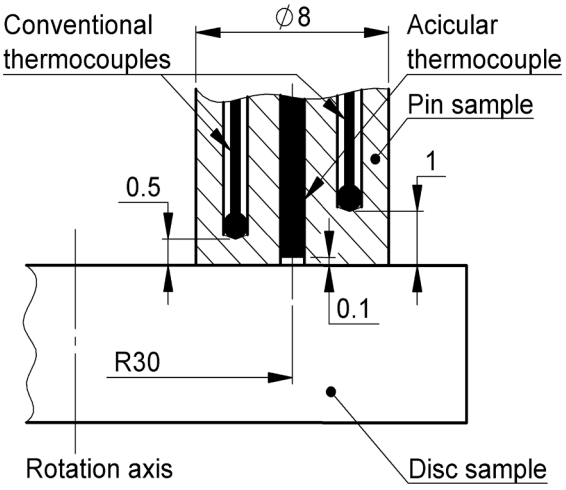

Fig. 2. Locations of the acicular and conventional thermocouples in the pin sample.

their measuring junctions and the friction surface were 0.5 mm and 1 mm. The measured temperature rise is denoted by $T_{CT0.5}$ and T_{CT1}, respectively. The liquid bath and furnace calibration tests confirmed the conventional thermocouples to have an absolute accuracy of ±1 °C in the temperature range of 0–150 °C.

The temperature signals T_{AGT}, $T_{CT0.5}$ and T_{CT1} were sampled by a Graphtech GL7000/GL7-HSV data logger. The sampling frequency and low-pass cutoff frequency were respectively set equal to 1 Hz and 1.5 Hz for the stationary regime and 10 Hz and 5 Hz for the transient regimes.

In addition to the acicular and conventional thermocouples, a Cedip Titanium 560 M infrared thermographic camera with detector spectral range of 3.6–5.1 μm, thermal sensitivity of 20 mK and resolution of 640 × 512 pixels was used. The thermal image was taken every 30 min for the stationary regime and at frequency 10 Hz for the transient regimes. An example of the thermal image is illustrated in Fig. 3. Analysis of the thermal image allowed determining the maximum temperature rise T_{IR} in the visible region of contact and the average temperature rise T_{cal} in the visible part of the pin sample (for calibration purpose). Note that the values of T_{IR} and T_{cal} should be considered as indicative due to uncertainty in the emissivity of the pin sample surface and the effect of reflected background radiation.

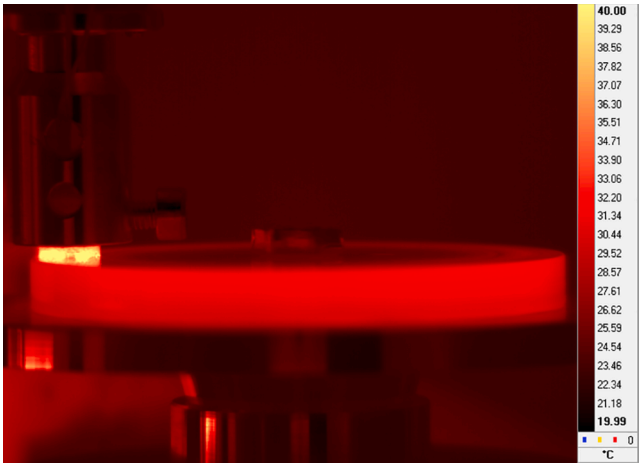

Fig. 3. Thermal image obtained by infrared thermography (brake pads material, velocity step).

Table 1
Properties of the tested materials.

Property	Copper	Brake pads material	Polyamide
Density, g/cm^3	8.9	2.6	1.1
Elastic modulus, GPa	130	10	2.5
Hardness	100 HBW 2.5/187.5	55 Shore D	51 Shore D
Thermal conductivity, W/(m °C)	390	0.77	0.26
Emissivity	0.75 (oxidised)	0.97	0.85

2.3. Friction materials

The disc samples were made of 42CrMo4 steel with hardness 180 HB. The pin samples were manufactured from three friction materials of various classes. The first material was a 99.9% copper. This metal is often used in sliding electrical contacts. The second material was a multi-ingredient friction material used in car brake pads. It contained about 14 wt% iron in the form of steel fibre. The third material was a PA6G polyamide used for manufacturing sliding contact bearings and rollers.

The relevant properties of the tested materials are given in Table 1. There is a decreasing trend in the density, elastic modulus, hardness and thermal conductivity for the sequence of copper – brake pads material – polyamide. Moreover, copper has drastically higher elastic modulus, hardness and thermal conductivity compared to the other materials. Note that the softer brake pads material and polyamide are characterised in Shore D hardness scale.

2.4. Regimes of friction

Each material was tested under four regimes of friction, as described in Table 2. The axial load on the pin sample was equal to 25 N for all regimes, which corresponded to the contact pressure of 0.5 MPa. In the stationary regime, the sliding velocity v (at the average friction radius) was constant. Three transient regimes were simulated differing in the behaviour of v, as shown in Fig. 4. The regime of velocity step implied a fast increase in v and maintaining its magnitude at a desired level. The regime of acceleration represented a nearly linear increase in v. The regime of deceleration implied a fast increase in v and subsequent nearly linear decrease in its magnitude. The values of the contact pressure, sliding velocity v and test duration were chosen in such a way as to provide sufficient temperature rise in the pin sample (in order to have temperature signal measurable with high accuracy); prevent excessive temperature rise (in order to minimise the temperature effects on the materials properties) and comply with the tribometer performance. The environment temperature was 20 ± 2 °C.

3. Results and discussion

3.1. Stationary regime

Fig. 5 presents the experimental data obtained under the stationary conditions for each material. The plot on the left shows the behaviour of the friction force F and linear wear δ, whilst the one on the right shows the temperature curves of T_{AGT}, $T_{CT0.5}$, T_{CT1} and T_{IR} measured by the acicular thermocouple, conventional thermocouple at 0.5 mm depth, conventional thermocouple at 1 mm depth and infrared camera, respectively.

Fig. 5a corresponds to the copper pin sample. It can be seen that F is stable during the test with a slight trend to increase its value. The value of δ initially decreases, which can be explained by the thermal expansion of the pin and disc samples, and then increases practically in a linear manner, indicating a constant wear rate. T_{AGT}, $T_{CT0.5}$, T_{CT1} and T_{IR} exhibit a typical transition to the stationary thermal state. T_{AGT} from the acicular thermocouple is about 5% higher than $T_{CT0.5}$, suggesting a more intensive heat generation in the contact region between the working part of the acicular thermocouple and the disc sample. T_{IR} registered by the infrared camera corresponds well with T_{AGT} as the stationary thermal state is reached. It is interesting that δ exceeds the 0.1 mm initial gap between the working part and friction surface, i.e. the acicular thermocouple gets involved in friction during the test. No qualitative changes can, however, be seen in the behaviour of T_{AGT}.

Fig. 5a also indicates that $T_{CT0.5}$ and T_{CT1} from the conventional thermocouples are hardly distinguishable, implying almost uniform temperature distribution in the pin sample. This result is expectable due

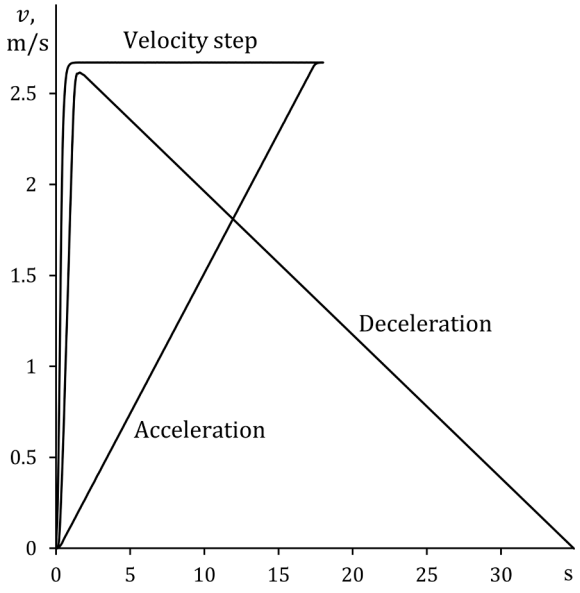

Fig. 4. Change in the sliding velocity v in the transient regimes.

Table 2
Regimes of friction.

Regime		Number of tests	Contact pressure	Sliding velocity v	Duration
Stationary friction		2	0.5 MPa	2 m/s	60–180 min
Transient friction	Velocity step	10	0.5 MPa	Increase from 0 to 2.7 m/s	1 s
				2.7 m/s	17 s
	Acceleration	10	0.5 MPa	Linear increase from 0 to 2.7 m/s	18 s
	Deceleration	10	0.5 MPa	Increase from 0 to 2.7 m/s	2 s
				Linear decrease from 2.7 m/s to 0	33 s

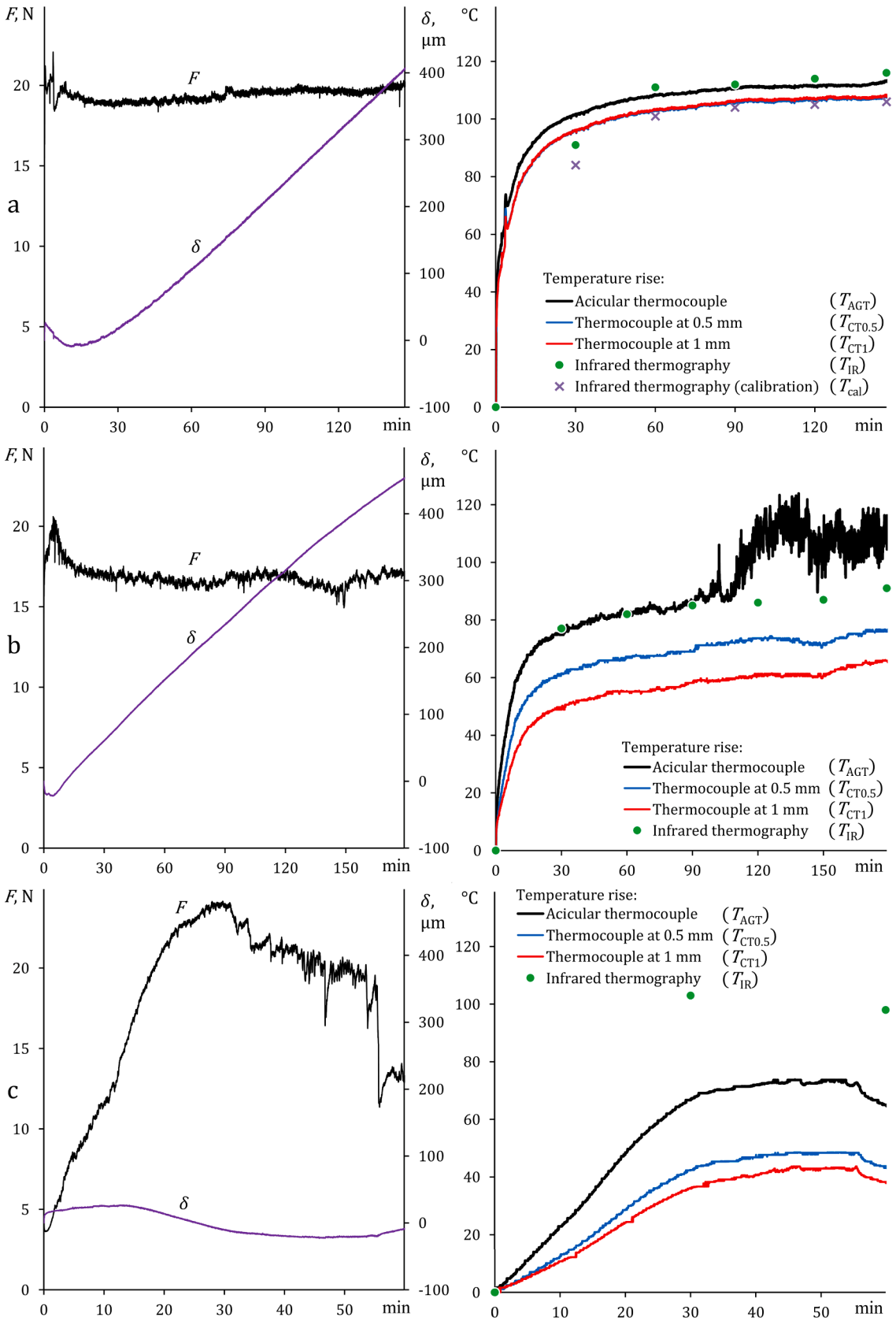

Fig. 5. Stationary regime: (a) copper; (b) brake pads material; (c) polyamide.

to a high thermal conductivity of copper (see Table 1). The average temperature rise T_{cal} in the visible part of the pin sample corresponds well with the temperature curve of $T_{CT0.5}$, which can be considered as a rough validation of T_{IR} obtained for the copper pin sample.

Further, Fig. 5b shows the experimental data for the brake pads material. Here the variations in F are more noticeable in comparison with the previous case, which is likely caused by the inhomogeneity of the brake pads material due to the presence of steel fibres in it. $T_{CT0.5}$ and T_{CT1} behave in a similar manner. There is about 13 °C difference between them due to a substantially lower thermal conductivity of the brake pads material compared to copper (see Table 1). T_{IR} follows the variations in $T_{CT0.5}$ exceeding it by about 15 °C. Since T_{IR} corresponds to the visible contact region, whilst $T_{CT0.5}$ and T_{CT1} are measured at respective depths 0.5 mm and 1 mm, the approximate equality of $T_{IR} - T_{CT0.5} \approx T_{CT0.5} - T_{CT1}$ implies a nearly linear temperature distribution (or, in other words, uniform heat flux) in the axial direction of the pin sample in the vicinity of the friction surface. T_{AGT} practically coincides with T_{IR} in the initial interval of time. At the instance of about 90 min, the acicular thermocouple gets involved in friction, whereafter T_{AGT} has an oscillatory character, exceeding T_{IR} by 18% on average. The oscillations in T_{AGT} are the result of multiple frictional interactions between the acicular thermocouple and disc sample.

Finally, Fig. 5c illustrates the relevant data for the polyamide pin sample. It can be seen that a transient process lasting approximately 30 min takes place. The value of F increases drastically. T_{AGT}, $T_{CT0.5}$ and T_{CT1} reach their stationary values in a similar manner. The difference between T_{IR} and T_{AGT}, between T_{AGT} and $T_{CT0.5}$, and between $T_{CT0.5}$ and T_{CT1} is about 33 °C, 23 °C and 6 °C, respectively. These values reveal a substantially non-linear temperature distribution in the axial direction of the pin sample in the vicinity of the friction surface. As regards δ, its non-monotonic behaviour is governed by the wear process, thermal expansion of the pin and disc samples, transfer of the polyamide from the pin sample to the disc sample, etc. Since the value of δ remains within ±26 μm, the acicular thermocouple does not get involved in friction during the test, which is also confirmed by the smooth change in T_{AGT} and after-test examination of the worn surfaces of the pin and disc samples. After about 50 min of the test, a significant drop of F can be seen, along with a decrease in T_{AGT}, $T_{CT0.5}$ and T_{CT1}, which can be explained by the glass–liquid transition in the polyamide (its glass-transition temperature is about 50 °C).

Thereby, stationary T_{AGT} corresponds well with T_{IR} for the copper pin sample. In the case of brake pads material, T_{AGT} is about 18% higher than T_{IR} for the acicular thermocouple involved in friction and coincides with T_{IR} otherwise. As regards the polyamide, no reliable quantitative conclusions can be reached here due to the complicated temperature data and unstable frictional behaviour of this material at higher temperatures.

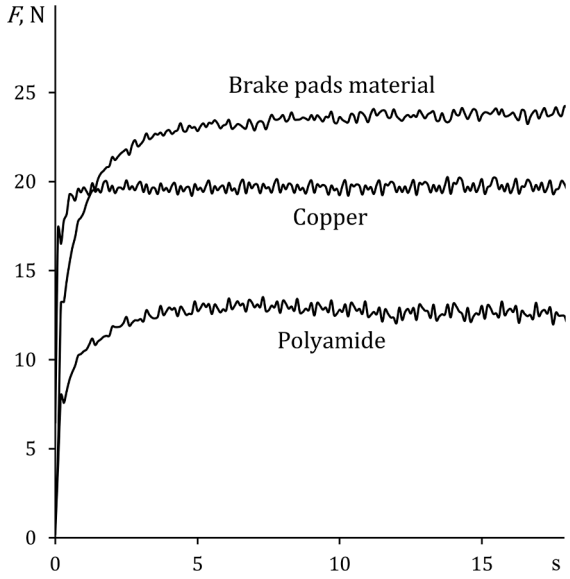

Fig. 6. Change in the friction force F in the regime of velocity step.

3.2. Transient regimes

The transient regimes are characterised by variable sliding velocity v, as described in Table 2 and Fig. 4. The studied materials exhibit stable behaviour of the friction force F in these regimes. For instance, Fig. 6 presents the change in F in the regime of velocity step. It can be seen that the value of F for the polyamide is noticeably smaller in comparison with the values for copper and the brake pads material. Accordingly, the polyamide on steel pair generates less friction heat.

Fig. 7 shows the transient temperature curves obtained for the copper pin sample. As it may be expected, the temperature curves of $T_{CT0.5}$ and T_{CT1} lie close to each other. Moreover, they are hardly distinguishable in the regime of velocity step. T_{IR} agrees surprisingly well with $T_{CT0.5}$, although being slightly lower for the regime of velocity step and slightly higher for the regimes of acceleration and deceleration. The behaviour of T_{AGT} is the most interesting. It can be seen that as compared to $T_{CT0.5}$, T_{AGT} is slightly higher for the regime of acceleration and considerably higher for the regimes of velocity step and deceleration. In the latter regime, T_{AGT} reaches its maximum with about 2 s delay with respect to $T_{CT0.5}$. Thereby, the mentioned deviation of T_{AGT} from $T_{CT0.5}$ is attributed to a more intensive heat generation in the contact region between the working part of the acicular thermocouple and disc sample along with the delay of T_{AGT}.

The liquid bath tests of the acicular thermocouple working part with diameter 0.41 mm showed that its response time is about 18 ms (Nosko et al. [27]). This value is comparable to those reported for the thermocouples of similar wire-in-hollow-cylinder constructions used in aerodynamic and hydrodynamic measurements (Mohammed et al. [30], Menezes and Bhat [31], Irimpan et al. [32], Manjhi and Kumar [36]). The 2 s delay of T_{AGT}, observed in the present study, characterises the thermal inertia of the acicular thermocouple, i.e. its response to variation in temperature at the sliding surface. This response is evidently slowed down by the thermal resistance at the interface between the working part and friction material.

Fig. 8 shows the temperature curves obtained for the brake pads material. In contrast to the previous case, T_{IR} oscillates with higher amplitude and is considerably higher than $T_{CT0.5}$. Such a behaviour of T_{IR} is attributed to a substantially lower thermal conductivity of the brake pads material compared to copper (see Table 1). T_{AGT} exhibit random peaks due to the multiple involvement of the acicular thermocouple in friction. In addition, a delay of T_{AGT} with respect to T_{IR} is seen in the regime of deceleration, similar to that for the copper pin sample (see Fig. 7). Despite the mentioned random variations in T_{AGT} and T_{IR} and delay of the former, there is acceptable agreement between these temperatures.

Fig. 9 shows the temperature curves obtained for the polyamide. It can be seen that $T_{CT0.5}$ and T_{CT1} take considerably smaller values compared to those for copper and the brake pads material, which is due to a very low thermal conductivity of the polyamide (see Table 1) along with a lower friction force F (see Fig. 6). The acicular thermocouple indicates abnormally high T_{AGT} that exceeds T_{IR} and $T_{CT0.5}$ by order of magnitude. This result can be explained by a low elastic modulus of the polyamide (see Table 1). During the test, the polyamide pin sample is subjected to a large axial deformation and, accordingly, a significant fraction of the normal load is transferred to the working part of the acicular thermocouple, which leads to a disproportionally intensive heat generation in the contact region between the working part and disc sample. Apparently, under the mentioned conditions the acicular thermocouple cannot provide reliable and accurate measurement. The polyamide is therefore excluded from the further consideration. Note

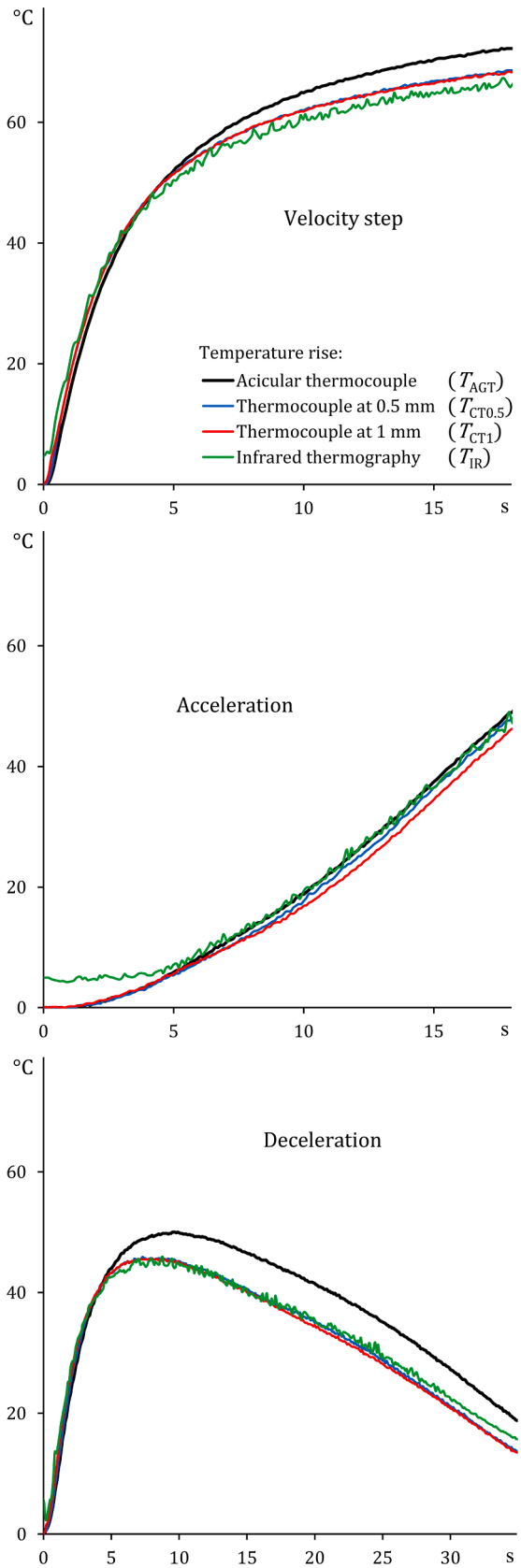

Fig. 7. Transient temperature curves of T_{AGT}, $T_{CT0.5}$, T_{CT1} and T_{IR} for copper.

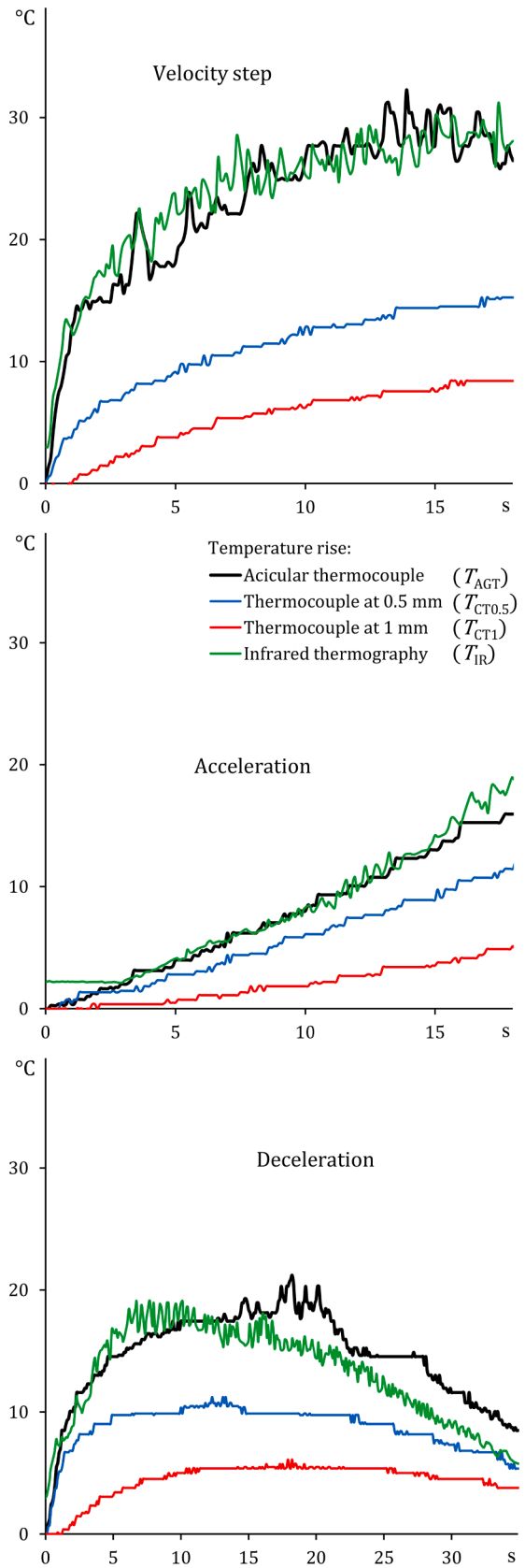

Fig. 8. Transient temperature curves of T_{AGT}, $T_{CT0.5}$, T_{CT1} and T_{IR} for the brake pads material.

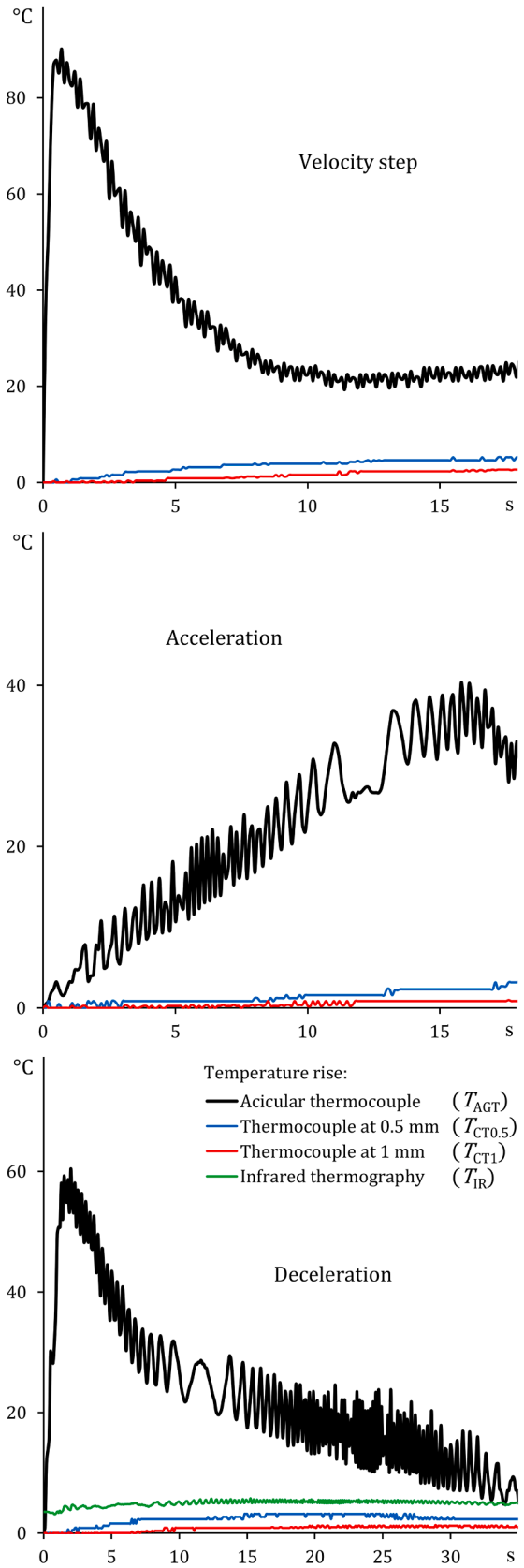

Fig. 9. Transient temperature curves of T_{AGT}, $T_{CT0.5}$, T_{CT1} and T_{IR} for the polyamide.

that due to technical reasons the temperature data of T_{IR} were not obtained in the regimes of velocity step and acceleration and, accordingly, are not presented in Fig. 9.

The experimental data from the test repetitions allow evaluating the test-retest reliability of the acicular thermocouple. Fig. 10 shows the temperature curves of T_{AGT} obtained in 3 consecutive tests of each transient regime. In the case of copper (Fig. 10a), the temperature curves agree well with each other. As regards the brake pads material (Fig. 10b), a larger scatter of the temperature curves occurs. There are individual peaks of T_{AGT} due to the involvement of the acicular thermocouple in friction, however, these peaks are relatively short in time and do not introduce a global distortion to the temperature curve.

The measurement accuracy of the acicular thermocouple is estimated with respect to the temperature rise T_{IR} registered by the infrared camera. Fig. 11 illustrates the mean relative deviation ε of T_{AGT} from T_{IR} during the test for the stationary and transient regimes. The top end of the bar indicates the mean value of ε, while the line segment indicates the standard deviation of ε across the tests. Within the transient regimes, ε makes up 7–15% for copper, whilst it is 10–19% for the brake pads material. The smaller deviation ε for copper can be explained by the fact that copper is significantly stiffer than the brake pads material (see Table 1) and, accordingly, the copper pin sample undergoes smaller axial deformations, implying a lower excessive normal load on the working part of the acicular thermocouple. It is remarkable that ε takes a larger value in the regime of deceleration for both copper and brake pads material, which is attributed to the thermal inertia of the acicular thermocouple.

Thus, the obtained findings suggest that the acicular thermocouple technique is applicable to stiffer friction materials, like copper or brake pads material, under stationary or slowly changing conditions. The technique applicability to short-duration transient regimes is limited by the thermal inertia of the acicular thermocouple characterised by about 2 s temperature response delay. This problem can be most probably overcome by developing acicular thermocouples that possess a smaller working part and reducing the thermal resistance between the working part and friction material. However, the possibility to extend the technique application to more pliable and softer materials, like polyamide, remains questionable and may be the subject of future studies.

4. Conclusions

The reliability and accuracy of the acicular grindable thermocouple technique were experimentally investigated for the friction materials of various classes, including copper, brake pads material and polyamide. The mentioned materials in the form of pin samples were tested against steel disc samples under stationary regime and three transient regimes, namely, velocity step, acceleration and deceleration. The measurement accuracy of the acicular thermocouple was estimated by comparing its signal T_{AGT} with the temperature rise T_{IR} registered by infrared thermography. The main findings of the study can be summarised as follows.

- Under the stationary regime, T_{AGT} agrees well with T_{IR} for copper, whilst T_{AGT} exceeds T_{IR} by about 18% when the acicular thermocouple is involved in friction for the brake pads material.
- In general, the measurements by the acicular thermocouples are test-retest reliable for copper and the brake pads material.
- Under the transient regimes, the mean relative deviation of T_{AGT} from T_{IR} makes up 7–15% for copper and 10–19% for the brake pads material.
- The thermal inertia of the acicular thermocouple is characterised by a temperature response delay of about 2 s. The delay is especially considerable in the regime of deceleration.
- The acicular thermocouple indicates abnormally high temperature for the polyamide, which is caused by the deformation of this relatively pliable material and associated transfer of a significant fraction of the normal load to the acicular thermocouple.

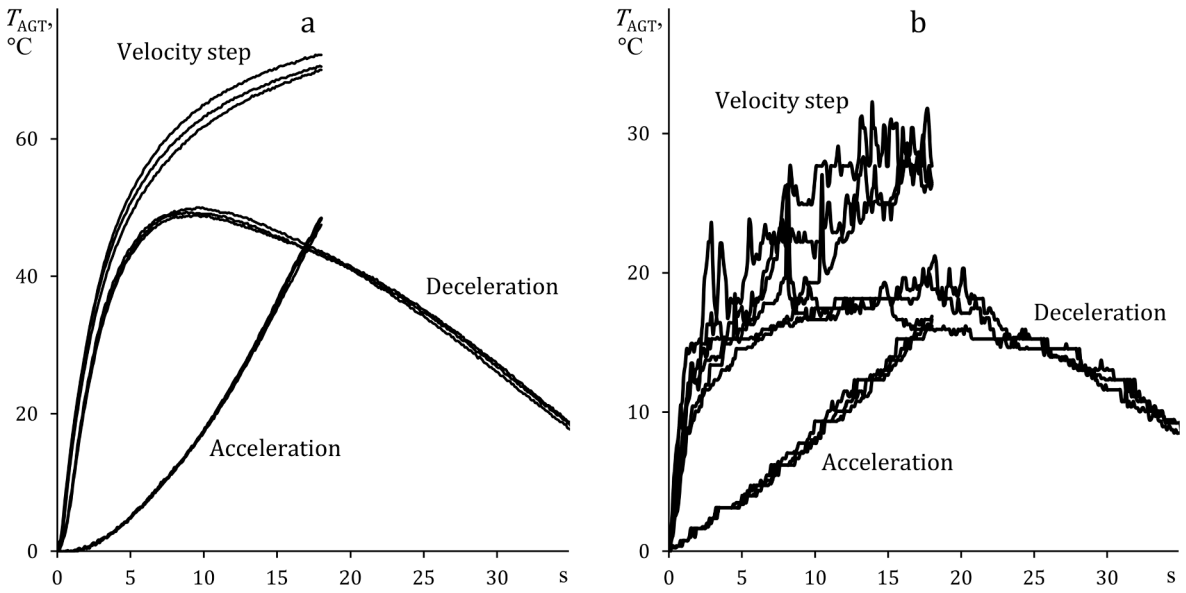

Fig. 10. Test-retest reliability of the acicular thermocouple: (a) copper; (b) brake pads material.

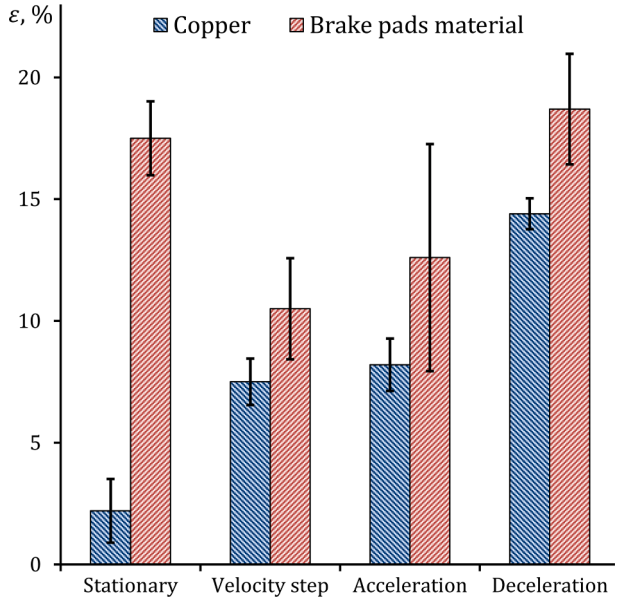

Fig. 11. Mean relative deviation ε of T_{AGT} from T_{IR} during the test.

CRediT authorship contribution statement

Oleksii Nosko: Funding acquisition, Supervision, Conceptualization, Writing – original draft. **Yurii Tsybrii:** Investigation, Validation, Writing – review & editing. **Wojciech Tarasiuk:** Methodology, Visualization, Software. **Andrey Nosko:** Supervision, Writing – review & editing.

Declaration of Competing Interest

The authors declare that they have no known competing financial interests or personal relationships that could have appeared to influence the work reported in this paper.

Acknowledgements

The authors wish to thank Dr Magdalena Łępicka, Dr Adam Adamowicz and Mr Wojciech Grodzki at Bialystok University of Technology for their assistance in conducting experiments.

Funding: This work was supported by the National Science Centre, Poland [grant number 2017/26/D/ST8/00142].

References

[1] F.E. Kennedy, Thermal and thermomechanical effects in dry sliding, Wear 100 (1-3) (1984) 453–476.
[2] R. Komanduri, Z.B. Hou, A review of the experimental techniques for the measurement of heat and temperatures generated in some manufacturing processes and tribology, Tribol. Int. 34 (10) (2001) 653–682.
[3] M.A. Davies, T. Ueda, R. M'Saoubi, B. Mullany, A.L. Cooke, On the measurement of temperature in material removal processes, Ann. CIRP 56 (2) (2007) 581–604.
[4] T.P. Newcomb, Transient temperatures in brake drums and linings, Proc. Instit. Mech. Eng.: Automob. Div. 12 (1) (1958) 227–244.
[5] Y.-C. Yang, W.-L. Chen, A nonlinear inverse problem in estimating the heat flux of the disc in a disc brake system, Appl. Therm. Eng. 31 (14-15) (2011) 2439–2448.
[6] J.G. Bauzin, M.N. Nguyen, N. Laraqi, M.B. Cherikh, Thermal characterization of frictional interfaces using experiments and inverse heat conduction methods, Int. J. Therm. Sci. 137 (2019) 431–437.
[7] O. Nosko, Y. Tsybrii, Inverse determination of sliding surface temperature based on measurements by thermocouples with account of their thermal inertia, Tribol. Int. 164 (2021), 107200.
[8] F.P. Bowden, K.E.W. Ridler, Physical properties of surfaces. III — The surface temperature of sliding metals. The temperature of lubricated surfaces, Proc. Roy. Soc. London A 154 (1936) 640–656.
[9] J. Peklenik, Ermittlung von geometrischen und physikalischen Kenngrössen für die Grundlagenforschung des Schleifens [dissertation], TH Aachen, 1957, Aachen. (in German).
[10] A.V. Yakimov, Y.A. Kazimirchik, V.A. Sipailov, Investigation of temperatures in the grinding zone, Russian Eng. J. (8) (1964) 64–66, in Russian.
[11] V.V. Tatarenko, G.D. Salo, B.Y. Borisov, Microthermocouples to investigate temperature fields in the grinding zone, Russian Eng. J. (1) (1969) 50–51, in Russian.
[12] V.G. Lebedev, R.A. Zhabokritskiy, Temperature in gear grinding by diamond and cubic boron nitride wheels, Machine Tools (10) (1969) 28–30, in Russian.
[13] I.P. Karaim, Measurement acuracy of the contact temperature in grinding using a thermoelectrode, Russian Eng. J. (5) (1970) 89, in Russian.
[14] A.Y.C. Nee, A.O. Tay, On the measurement of surface grinding temperature, Int. J. Mach. Tool Des. Res. 21 (3-4) (1981) 279–291.
[15] W.B. Rowe, S.C.E. Black, B. Mills, H.S. Qi, M.N. Morgan, Experimental investigation of heat transfer in grinding, CIRP Ann. 44 (1) (1995) 329–332.
[16] D. Babic, D.B. Murray, A.A. Torrance, Mist jet cooling of grinding processes, Int. J. Mach. Tools Manuf. 45 (10) (2005) 1171–1177.
[17] A.D. Batako, W.B. Rowe, M.N. Morgan, Temperature measurement in high efficiency deep grinding, Int. J. Mach. Tools Manuf. 45 (11) (2005) 1231–1245.
[18] A. Lefebvre, P. Vieville, P. Lipinski, C. Lescalier, Numerical analysis of grinding temperature measurement by the foil/workpiece thermocouple method, Int. J. Mach. Tools Manuf. 46 (14) (2006) 1716–1726.
[19] A. Lefebvre, F. Lanzetta, P. Lipinski, A.A. Torrance, Measurement of grinding temperatures using a foil/workpiece thermocouple, Int. J. Mach. Tools Manuf. 58 (2012) 1–10.

[20] L.M. Barczak, A.D.L. Batako, M.N. Morgan, A study of plane surface grinding under minimum quantity lubrication (MQL) conditions, Int. J. Mach. Tools Manuf. 50 (11) (2010) 977–985.
[21] X. Tian, F.E. Kennedy, J.J. Deacutis, A.K. Henning, The development and use of thin film thermocouples for contact temperature measurement, Tribol. Trans. 35 (3) (1992) 491–499.
[22] F.E. Kennedy, D. Frusescu, J. Li, Thin film thermocouples arrays for sliding surface temperature measurement, Wear 207 (1997) 46–54.
[23] V.I. Guskov, A new method of temperature measurement in the grinding zone, Russian Eng. J. (6) (1974) 74–75, in Russian.
[24] A.M. Romashko, Study of heating of lift-and-transport machines disk brakes [dissertation], Bauman Moscow Higher Technical School, 1979, Moscow. (in Russian).
[25] A.L. Nosko, Y. Kimura, Surface temperature measurement with tape-type thermocouples, Proceedings of the 6th Nordic Symposium on Tribology NORDTRIB94, 1994, Uppsala, p. 613–620.
[26] O. Nosko, T. Nagamine, A.L. Nosko, A.M. Romashko, H. Mori, Y. Sato, Measurement of temperature at sliding polymer surface by grindable thermocouples, Tribol. Int. 88 (2015) 100–106.
[27] O. Nosko, W. Tarasiuk, Y. Tsybrii, A. Nosko, A. Senatore, V. D'Urso, Performance of acicular grindable thermocouples for temperature measurements at sliding contacts, Measurement 181 (2021), 109641.
[28] W. Tarasiuk, Y. Tsybrii, O. Nosko, A. Nosko, Accuracy and transparency of sliding surface temperature measurements by acicular grindable thermocouples, in: Proceedings of the 20th International Symposium INFOTEH-JAHORINA, 17–19 March 2021, East Sarajevo, 9400704, doi: 10.1109/INFOTEH51037.2021.9400704.
[29] H. Mohammed, H. Salleh, M.Z. Yusoff, Design and fabrication of coaxial surface junction thermocouples for transient heat transfer measurements, Int. Commun. Heat Mass Transfer 35 (7) (2008) 853–859.
[30] H.A. Mohammed, H. Salleh, M.Z. Yusoff, Determination of the effusivity of different scratched coaxial temperature sensors under hypersonic flow, Int. J. Thermophys. 31 (11-12) (2010) 2305–2322.
[31] V. Menezes, S. Bhat, A coaxial thermocouple for shock tunnel applications, Rev. Scientific Instrum. 81 (2010) 104905.
[32] K.J. Irimpan, N. Mannil, H. Arya, V. Menezes, Performance evaluation of coaxial thermocouple against platinum thin film gauge for heat flux measurement in shock tunnel, Measurement 61 (2015) 291–298.
[33] S. Agarwal, N. Sahoo, R.K. Singh, Experimental techniques for thermal product determination of coaxial surface junction thermocouples during short duration transient measurements, Int. J. Heat Mass Transf. 103 (2016) 327–335.
[34] S.L.N. Desikan, K. Suresh, K. Srinivasan, P.G. Raveendran, Fast response co-axial thermocouple for short duration impulse facilities, Appl. Therm. Eng. 96 (2016) 48–56.
[35] J. Li, H. Chen, S. Zhang, X. Zhang, H. Yu, On the response of coaxial surface thermocouples for transient aerodynamic heating measurements, Exp. Therm. Fluid Sci. 86 (2017) 141–148.
[36] S. Manjhi, R. Kumar, Transient surface heat flux measurement for short duration using K-type, E-type and J-type of coaxial thermocouples for internal combustion engine, Measurement 136 (2019) 256–268.
[37] S. Manjhi, R. Kumar, Performance analysis of coaxial thermocouples for heat flux measurement of an aerodynamic model on shock tube facility, Measurement 166 (2020), 108221.
[38] A.K. Rout, N. Sahoo, P. Kalita, Effectiveness of coaxial surface junction thermal probe for transient measurements through laser based heat flux assessment, Heat Mass Transf. 56 (4) (2020) 1141–1152.